


Pressure and Flow Rate Changes During Contrast Injections in Cerebral Angiography: Correlation to Reflux Length

BRANDON KOVAROVIC,¹ HENRY H. WOO,² DAVID FIORELLA,² BARUCH B. LIEBER,^{1,2}
and CHANDER SADASIVAN ²

¹Department of Biomedical Engineering, Stony Brook University, 102 Bioengineering Building, Stony Brook, NY 11794-5281, USA; and ²Department of Neurological Surgery, Stony Brook University, HSC T-12, Rm 080, Stony Brook, NY 11794-8122, USA

(Received 17 July 2017; accepted 22 February 2018; published online 1 March 2018)

Associate Editor David Elad and Ajit P. Yoganathan oversaw the review of this article.

Abstract—Cerebral angiography involves the antegrade injection of contrast media through a catheter into the vasculature to visualize the region of interest under X-ray imaging. Depending on the injection and blood flow parameters, the bolus of contrast can propagate in the upstream direction and proximal to the catheter tip, at which point contrast is said to have refluxed. In this *in vitro* study, we investigate the relationship of fundamental hemodynamic variables to this phenomenon. Contrast injections were carried out under steady and pulsatile flow using various vessel diameters, catheter sizes, working fluid flow rates, and injection rates. The distance from the catheter tip to the proximal edge of the contrast bolus, called reflux length, was measured on the angiograms; the relation of this reflux length to different hemodynamic parameters was evaluated. Results show that contrast reflux occurs when the pressure distal to the catheter tip increases to be greater than the pressure proximal to the catheter tip. The ratio of this pressure difference to the baseline flow rate, called reflux resistance here, was linearly correlated to the normalized reflux length (reflux length/vessel diameter). Further, the ratio of blood flow to contrast fluid momentums, called the Craya–Curtet number, was correlated to the normalized reflux length *via* a sigmoid function. A sigmoid function was also found to be representative of the relationship between the ratio of the Reynolds numbers of blood flow to contrast and the normalized reflux length. As described by previous reports, catheter based contrast injections cause substantial increases in local flow and pressure. Contrast reflux should generally be avoided during standard antegrade angiography. Our study shows two specific correlations between contrast reflux length and baseline and intra-injection parameters that have not been published previously. Further studies need to be conducted to fully characterize the phenomena and to extract reliable indicators of clinical utility. Parameters relevant to

cerebral angiography are studied here, but the essential principles are applicable to all angiographic procedures involving antegrade catheter injections.

Keywords—Reflux length, Efflux length, Craya–Curtet number, Pressure gradient, Reflux resistance, Logistic function.

INTRODUCTION

X-ray angiography is the technique of injecting a contrast medium through a catheter into the vasculature to mix with the blood and opacify the geometry of the vasculature under radiographic imaging. Cerebral angiography remains the gold-standard imaging modality for diagnosis as well as treatment of cerebrovascular pathologies. It is routinely used by neuro-interventionalists to identify cerebral aneurysms and other pathologies in the cerebral vasculature. It is used at every step in minimally-invasive endovascular treatment including diagnosis, intra-operative imaging, as well as treatment follow-up. Since the advent of angiography 90 years ago, a vast body of literature has been accumulated to extract functional information from the imaging.²² Most studies have extracted blood flow measures based on transit time³⁴ or indicator dilution¹³ methods. Others have investigated post-injection hemodynamic recovery and systemic hemodynamics such as the effect of ionic content and toxicity of the contrast medium or delayed vasodilation of the capillary bed post-injection.^{12,14,25,30,44} However, the number of studies investigating flow and pressure changes during the contrast injection time period are relatively sparse.^{20,21,23,24,26,31,41,42} Scarcer still are

Address correspondence to Chander Sadasivan, Department of Neurological Surgery, Stony Brook University, HSC T-12, Rm 080, Stony Brook, NY 11794-8122, USA. Electronic mail: csadasivan@sbumed.org

investigations of the hemodynamics at and around the catheter tip.^{23,24}

Contrast media injections into laminar pipe-flow of blood result in complex physical phenomena. The relatively high injection flow rates through relatively small catheter diameters produce large velocities exiting the catheter that result in a jet with high Reynolds number (Re) flow. A 2.5 cc/s injection through a 2.4F catheter would, for example, result in a Re of 2260 or a 10 cc/s injection through a 5F catheter would result in a Re of 4970. This jet extends a certain length into the vessel, after which its energy is dissipated while mixing with blood *via* complex vortical flow structures or a turbulent spread over a certain length of the vessel. This mixing has previously been shown to be complete approximately ten vessel diameters from the catheter tip.²³ If the injection rates are too slow, the contrast will simply exit the catheter in a laminar stream and will not form a bolus that opacifies the lumen of the vascular geometry. Many previous analytical and *in vitro* studies have studied the complex development of (turbulent) jets inside enclosed laminar flow (coaxial confined jets), but in the context of chemical and aerospace engineering applications (ejector designs, combustor designs, *etc.*)^{16,18,29,35,43,46} and not for angiographic injections. The studies that have measured hemodynamics during contrast injections^{20,21,23,42} have noted substantial increases in flow and pressure distal to the catheter tip. Levin *et al.*²¹ found, for example, that injections of arterial blood (not iodinated contrast) into coronary and superior mesenteric arteries of dogs through a 7F catheter at 4–7 cc/s resulted in nearly 200% increases in the distal blood flow rates. This effect was reproduced even when saline was the injectate showing that the effect is hydraulic rather than biochemical (such as vasodilatory effects from red cell lysis).^{21,42}

Analytical solutions to describe the hemodynamics of contrast injections have been attempted by considering the system as lumped proximal and distal resistors as done by Morris and Walike²⁶ but their simplistic solution fails to account for distal flow increases during the injection as seen in their *in vitro* testing. A more complex analytical solution utilizing a 1-D wave propagation model in the entire circle of Willis by Mulder *et al.*²⁷ showed a minimal distal flow increase of up to 10% during contrast injections with almost no pressure increases, contrary to previous *in vivo* and clinical measurements.^{20,31,41} Recent computational fluid dynamics (CFD) techniques to study contrast injections primarily focus on virtual angiography models, where the goal is to capture the simulated front of the bolus and contrast concentrations in an attempt to extract the hemodynamics inside the vessel.^{7,8,38,40} These studies utilize laminar flow

assumptions, passive advection–diffusion transport of the contrast, and do not focus on the turbulent phenomenon at the catheter tip. Hao and Lieber used turbulent CFD techniques to characterize the concentration of contrast antegrade to the catheter tip to determine a proper mixing length.¹¹ The study did not capture any reflux behavior from the simulations. Proper CFD characterization of the turbulent jet behavior would be extremely computationally expensive with full transient turbulent simulations of two phase flow under pulsatile conditions. To that end, *in vitro* experiments allow a broader range of study variables with less effort as well as fewer simplifying assumptions such as a stationary catheter geometry or axisymmetric domains. Overall, although angiography is a common procedure, the development characteristics of the contrast bolus at and around the catheter tip and the concomitant hemodynamic changes in the vasculature have been poorly investigated due to the mechanical complexity of the phenomenon.

Clinically, hemodynamic changes during contrast injections are observed due to the inadvertent effect on distal pathologies. In the context of cerebral angiography, for example, there is a small risk of intra-angiography rupture or re-rupture of cerebral aneurysms due to increased pressure, with authors reporting 1.4–3.1% complication rates.^{32,33} The occurrence seems relatively rare and is mostly reported through case studies of re-rupture events.^{3,47} Dublin and French analyzed 30 case studies showing a predominance of female patients (71%) and 11 out of 14 patients had pre-angiographic hypertension.⁵ More recently, Kusumi *et al.*¹⁹ observed a statistically increased risk of aneurysm re-rupture during angiography when angiography was performed within 3 h of the initial hemorrhage. They found no significant difference in sex, blood pressure and age as compared to the group with re-rupture when angiography was not being performed.¹⁹

As mentioned, when contrast is injected in an antegrade fashion in blood vessels, a jet of contrast issues from the catheter tip and a hemodynamically complex mixing zone is established at, and immediately distal to, the catheter tip. The contrast medium completely opacifies the vessel diameter at the mixing zone forming a ‘bolus’ with proximal (lagging) and distal (leading) edges. As the contrast continues to be injected, the mixing bolus grows, extending both downstream/distally and upstream/proximally. Traditionally, when the contrast bolus grows such that the proximal edge of the bolus extends proximal to the catheter tip (Fig. 1, also Online Resource video), ‘contrast reflux’ is said to have occurred. Reflux is a notable property since the contrast bolus appears to flow upstream from both blood and injection flow and

beyond the entrance of the higher energy injection flow. We can define another phrase, ‘contrast efflux’, which occurs when the proximal edge of the bolus stays distal to the catheter tip (Fig. 1, also Online Resource video) throughout the injection period. Efflux and reflux can be quantified simply by measuring the distance between the catheter tip and the proximal edge of the contrast bolus. Although a handful of reports have evaluated contrast reflux in the context of hemodynamics,^{6,10} we are not aware of any studies that have quantified the hemodynamic conditions causing contrast reflux in antegrade catheter-based injections. In this *in vitro* study, we use various contrast injection scenarios to evaluate the relationship between pre- as well as intra-injection hemodynamics and contrast reflux. The rationale behind conducting the study was two-fold: (a) studying the impact of contrast injections might help establish contrast injection guidelines for physicians to reduce any complications such as aneurysm rupture, and (b) the potential ability to deduce changes in vascular hemodynamics from simple radiographic visualization of contrast reflux at the injection site might serve as an invaluable tool.

METHODS

The experiments involved contrast injections at varying injection rates through different catheters into straight tubes of varying diameter under both steady and pulsatile flow with simultaneous angiographic imaging, and flow and pressure measurements (Fig. 2). The distance from the catheter tip to the proximal edge of the bolus was measured on the angiograms with the catheter tip as the origin point along the vessel axis,

i.e., the negative direction represented reflux and the positive direction represented efflux (Fig. 1). The phrase ‘reflux length’ is used to describe both positive and negative directions throughout the manuscript. Four hemodynamic variables based on the flow and pressure measurements were then correlated to this reflux length. The experimental setup including the steady and pulsatile flow systems and the hemodynamic variables correlated to reflux length are described in detail below.

Experimental Setup

The testing setup was mounted to a rigid platform allowing consistent and level fixture of the tubes, catheters, pressure and flow sensors. Three straight tubes of 4.8, 6.35, and 8 mm diameter, all with a length of 40 cm, were used as the test vessel. The test vessels were made from Tygon[®] 2375 (Saint-Gobain Performance Plastics Inc., Courbevoie, France), which is fairly rigid (Shore 75A) to reduce any variability from compliance. The flow loop was constructed with 1/4" ID Tygon[®] 2375 tubing. The test vessels were mounted between two ‘T’ barb connectors with a 1/16" barb perpendicular to the flow allowing static pressures to be recorded 20 cm distal and 20 cm proximal to the catheter tip, *i.e.*, the catheter tip was always positioned at the mid-point of the test vessel. One pressure transducer (Validyne DP15, Validyne Engineering, Northridge, CA USA) was mounted to directly record the proximal pressure and the other pressure transducer (Validyne DP15) was mounted to record the pressure difference by connecting to both pressure taps; this ensured the pressure gradient was accurately recorded. An inline flow sensor (MPX6, Transonic Inc., Ithaca, NY USA) was mounted 30 cm downstream from the distal pressure tap. The

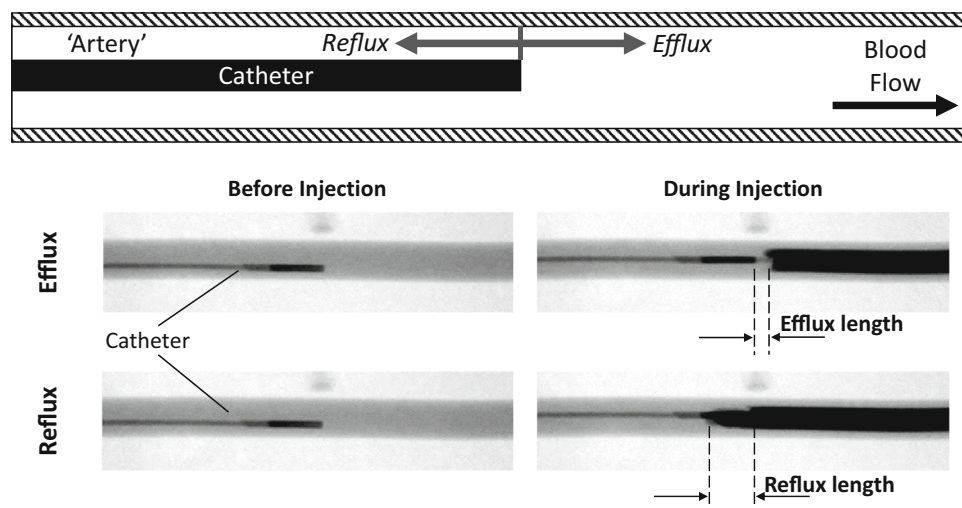


FIGURE 1. Sketch above and angiograms below explaining ‘reflux’ and ‘efflux’ during anterograde contrast injections into arteries. The corresponding lengths are measured between the catheter tip and the proximal edge of the contrast bolus.

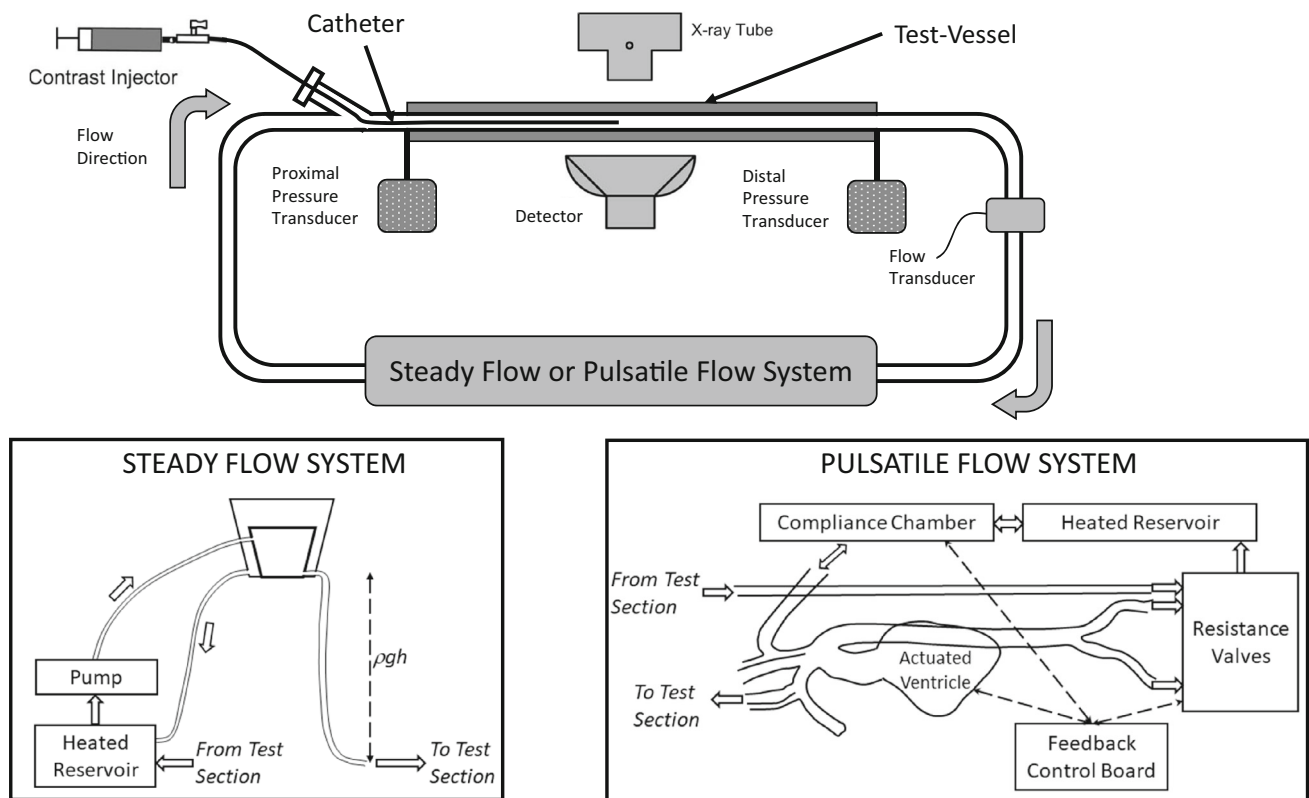


FIGURE 2. Schematic of the experimental flow rig; bottom schematics show some details of the steady and pulsatile flow systems.

flow and pressure sensors were calibrated each time the test vessel was changed. Pressures and flows were recorded with a PowerLab DAQ (ADInstruments Inc., Sydney, Australia) and LabChart software at 1000 samples/s. The flow and pressure data were processed with a custom script in MATLAB® (Mathworks Inc., Natick, MA USA).

A glycerol solution (50% by mass, 1.1 g/cc density, 3.4 cP viscosity at 37 °C) was used as the blood analogue (working fluid) and the injection medium was a solution (50/50 by volume) of Omnipaque® 300 (Iohexol, GE Healthcare Inc, Princeton, NJ USA) and 0.9% saline. The injection medium had a density of 1.16 g/cc and a viscosity of 2.02 cP at 25 °C. The injections were performed with a Medrad power-injector connected to a straight tip 4F or 5F Soft-Vu® catheter (Angiodynamics, Latham, NY USA) via high-pressure injection tubing. Four ml of contrast solution was injected at 3, 5, 6, 7, and 9 cc/s through the two different catheters in the steady flow system and 8 mL of contrast solution was injected at 3, 6, and 9 cc/s through the two different catheters in the pulsatile flow system (Table 1). The glycerol reservoir was maintained at 37 °C and replaced after 150 cc of contrast solution was injected to mitigate changes in the working fluid after repeated contrast injections.

Digital subtraction angiography (DSA) images were acquired with an Artis Zeego (Siemens Healthcare GmbH, Erlangen, Germany) at 7 frames/s. The test vessel was positioned in the center of the angiographic images (48 cm field of view). The X-ray source and detector were brought as close together as possible to reduce scatter and capture the highest contrast images with the largest field of view. Contrast injections were set to a 1 s delay after initial imaging to obtain the proper mask for the DSA images. Images were acquired till the injected volume had washed out of the field of view. Measurement of the contrast reflux and efflux lengths (Fig. 1) was done directly on the Artis Zeego workstation after appropriate calibration based on the diameter of the test vessel.

Steady Flow System

Steady flow was obtained with a constant pressure-head, gravity-feed, system utilizing a continuously overflowing container (Fig. 2). The container was fed with a small peristaltic pump pulling from a heated reservoir. Feed tubing and volume displaced by the pump was kept at a minimum to reduce any noise in the flow. The container was affixed to a height-adjustable platform to consistently generate different

TABLE 1. Study parameters used for the steady and pulsatile flow systems.

Variable	Steady flow	Pulsatile flow
Test vessel inner diameter	4.8, 6.35, 8 mm	4.8, 6.35, 8 mm
Catheter size	4F, 5F	4F, 5F
Injection volume	4 cc	8 cc
Injection rate	3, 5, 6, 7, 9 cc/s	3, 6, 9 cc/s
System flow and pressure ranges	Flows 1.5–3.5 cc/s Pressure 20–60 mmHg	Flows 2.5–5.5 cc/s Pressure 100–110 mmHg

There were a total of 81 conditions for steady flow and 49 conditions for pulsatile flow. The length of the test vessel was constant (40 cm) for all conditions.

flow rates and systemic pressures in the system by adjusting the height of the container relative to the angiography table (on which the test vessel rested). Approximately 10 different flow and pressure scenarios were evaluated with baseline flow rates ranging from 1.5 to 3.5 cc/s and pressures ranging from 20 to 60 mmHg (Table 1).

Pulsatile Flow System

Pulsatile flow was achieved with the Replicator[®] (Vascular Simulations, Stony Brook, NY, USA). The Replicator system is a pulsatile waveform diaphragm pump (with a functional left heart system) with a continuously adjusting Windkessel model and a physiologically accurate silicone model of the aortic tree (Fig. 2). The system automatically adjusts the arterial and venous compliance *via* feedback control of air column heights to achieve physiological systemic pressures of 120/80 mmHg. The heart rate was fixed at 70 BPM and cerebral flow rate was adjusted to 12 cc/s. The system has four cerebral inlets (left and right common carotid and left and right vertebral arteries), all of which connect to one cerebral outflow that is feedback-controlled.

The test vessel was connected to the right common carotid artery of the Replicator. Pinch valves were placed distal to the test segment in order to vary resistance and thus flow and pressure. Different flow scenarios were created by matching flow rates in the test vessel and adjusting the resistances of the arteries independently. The following scenarios were tested: baseline flow of 2.5 cc/s at 100 mmHg, 2.5 cc/s at 110 mmHg mean pressure and 5.5 cc/s at 100 mmHg mean pressure. Table 1 summarizes the pressure and flow ranges evaluated.

Hemodynamic Parameters

The following four hemodynamic variables were calculated from the baseline and intra-injection flow and pressure recordings and correlated to the contrast reflux lengths:

1. Pressure difference (mmHg): The time averaged difference between the proximal and distal pressures during the injection ($\Delta P = \overline{P_{\text{proximal}} - P_{\text{distal}}}|_{\text{injection}}$).
2. Reflux Resistance (mmHg s/cc): Contrast reflux is dependent on ΔP as well as the vascular resistance proximal to the catheter tip. This effect was deemed here as “Reflux Resistance” and quantified as the ratio of ΔP and the baseline mean blood flow rate (Eq. 1).

$$\text{Reflux Resistance} = \frac{\overline{P_{\text{proximal}} - P_{\text{distal}}}|_{\text{injection}}}{Q_{\text{blood, baseline}}} \quad (1)$$

3. Craya–Curtet number (dimensionless): This number, which is a ratio of the working fluid and contrast jet fluid momentums, was previously developed to characterize the mixability of a jet entering a confined flow.² The number has also been used to characterize contrast injections in the vasculature^{23,24} and was hypothesized to correlate to the observation of contrast reflux.²³ The Craya–Curtet number (Ct number) is defined in Eq. (2) where ρ_b and ρ_c are respectively the density of the blood/working fluid and the contrast medium, Q_b and Q_c are the flow rates of the blood and contrast, ID_{catheter} is the inner diameter of the catheter, ID_{vessel} is the inner diameter of the vessel and OD_{catheter} is the outer diameter of the catheter.

$$Ct = \left(\frac{\rho_b}{\rho_c}\right)^{\frac{1}{2}} \left(\frac{Q_b}{Q_c}\right) \left[\frac{ID_{\text{catheter}}}{(ID_{\text{vessel}}^2 - OD_{\text{catheter}}^2)^{\frac{1}{2}}} \right] \quad (2)$$

4. Ratio of Reynolds numbers (dimensionless): While the Craya–Curtet number is a ratio of the fluid momentums, the ratio of Reynolds numbers of the blood and the injection (Re

ratio, Eq. (3)) was also compared. The Re is a non-dimensional comparison of the inertial and viscous forces in the flow and therefore the Re ratio will look at forces as well as factor in the viscous component of the fluids. μ_b and μ_c are the viscosity of blood and contrast, respectively. The other variables are as defined above. The length scale chosen was the inner diameter of the catheter for the injection Re and the distance between the outer wall of the catheter and the vessel lumen for the blood Re (blood flow velocity is determined based on the annular cross-sectional area).

$$\frac{Re_b}{Re_c} = \frac{\rho_b Q_b \mu_c (ID_{\text{vessel}} - OD_{\text{catheter}}) ID_{\text{catheter}}}{\rho_c Q_c \mu_b (ID_{\text{vessel}}^2 - OD_{\text{catheter}}^2)} \quad (3)$$

Curve-fitting was accomplished using MATLAB Curve Fitting Toolbox. Outliers were not removed from the dataset. Fitting was done based on least-square regression resulting in R^2 values. Statistical analysis was conducted using GraphPad Instat (GraphPad software, La Jolla, CA).

RESULTS

Figure 3 shows typical pressure and flow waveforms for both steady and pulsatile scenarios. Pressure and flow data was processed in a MATLAB program designed to find the peak of the distal pressure waveform to identify the injection time period. The period of injection was determined based on the injection volume and flow rate (volume/flow rate). An additional 1.0 s of data before the peak was considered part of the injection to account for the rapid ramp of injection pressure (injection time period (s) = 1 + volume/flow rate). Baseline data was collected approximately 5 s before the injection and was averaged over 3 cardiac cycles or 2.5 s.

Observing the pressure and flow waveforms in both flow conditions, it is seen that the injection induces a dramatic increase in all the pressures and flows (Table 2). The average and maximum pressures during the injection show a unique feature of the contrast injection because *the distal pressure*, which is normally lower than proximal pressure to maintain forward flow, *increased to be more than the proximal pressure* (except in the steady flow average). Distal pressures also increased more than proximal pressures when compared to the corresponding baseline values (Table 2, % increase over baseline). Under the tested

conditions (Table 1), the difference between the maximum distal pressure during injection and the average distal pressure during injection was 9.3 ± 4.4 mmHg for the steady flow and 19.3 ± 13.8 mmHg for the pulsatile flow.

Table 2 also shows that while the injection rates were equal or larger than the baseline flows, the increased flow rates did not double, *i.e.*, the injection flow rate did not add to the blood flow rate during the injection. Integrating the increase during the injection did not yield the volume of the injection either. Since the power injector did not reach its set maximum pressure (break pressure) of 500 psi in the catheter, the flow rate of the injection should have remained constant and therefore the blood flow was restricted during the injection. We found no obvious correlations between system or injection parameters to the proximal or distal pressure magnitudes during injection. For example, Fig. 4 shows a plot of the injection velocity against maximal distal pressure during injections in the pulsatile flow system ($R^2 = 0.01$, $p = 0.41$). Table 3 shows differences and correlations of the increase in distal pressure over the baseline compared to catheter sizes, vessel diameters, baseline blood flow rate, baseline distal pressure, and injection velocity for both the steady and pulsatile flow systems. As can be noted, there are no strong correlations or physically relevant trends to the data. The only parameter to show statistical significance in both the steady and pulsatile flow systems is the catheter size, where there is a strong significance ($p < 0.0001$) under steady flow but a weak significance ($p = 0.045$) in the pulsatile system.

The injection rates and flow scenarios chosen for the study resulted in a wide range of reflux cases and a sufficient range of efflux cases. Under the tested conditions (Table 1), the steady flow system had average reflux lengths of -12.5 ± 23.0 mm and the pulsatile system had reflux lengths of -22.6 ± 32.5 mm. Table 3 shows differences and correlations of the reflux length compared to catheter sizes, vessel diameters, baseline blood flow rate, baseline distal pressure, and injection velocity for both the steady and pulsatile flow systems. The baseline blood flow rate and the baseline distal pressure are the only two parameters to show statistically significant correlations, but these correlations are extremely weak ($R^2 = 0.1$ for pulsatile flow). Thus, again, no strong, physically relevant trends can be noted. However, the pressure difference between the distal and proximal sites linearly correlated with the reflux lengths in both systems ($n = 81$, $R^2 = 0.44$, $p < 1E-4$ for steady flow; $n = 49$, $R^2 = 0.33$, $p < 1E-4$ for pulsatile flow) where greater pressure differences resulted in larger reflux lengths.

The reflux resistance linearly correlated to the reflux length ($n = 81$, $R^2 = 0.76$, $p < 1E-4$ for steady flow;

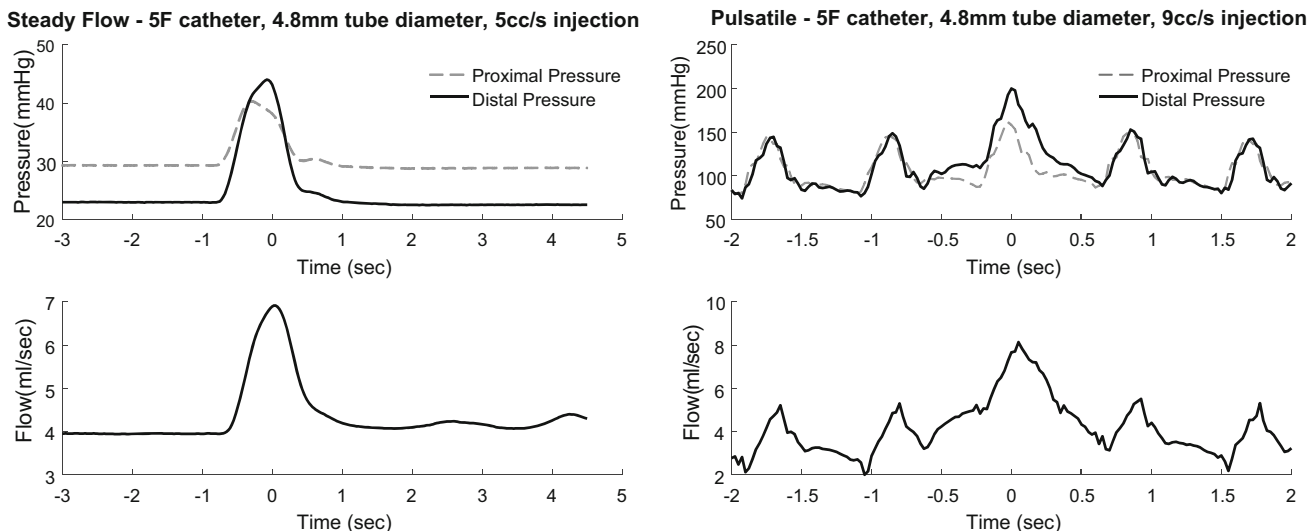


FIGURE 3. Typical examples of pressures and flow waveforms before, during, and after contrast injection under steady (left) and pulsatile (right) flow.

TABLE 2. Average ± standard deviation of pressures and flows during contrast injection under steady and pulsatile flow.

	Proximal pressure (mmHg)	Distal pressure (mmHg)	Flow rate (cc/s)
Steady flow			
Baseline	35.5 ± 11.5	32.0 ± 11.5	3.5 ± 1.6
Average during injection (% increase over baseline)	37.9 ± 12.2 (10.7 ± 6.9%)	36.5 ± 12.0 (15.9 ± 7.5%)	4.3 ± 1.9 (23.3 ± 12.5%)
Maximum during injection (% increase over baseline)	44.3 ± 13.4 (30 ± 8.2%)	45.8 ± 13.8 (47.1 ± 17.6%)	5.0 ± 2.1 (44.3 ± 19.3%)
Pulsatile flow			
Baseline	102.8 ± 2.6	102.2 ± 3.8	3.7 ± 1.4
Average during injection (% increase over baseline)	108.3 ± 3.5 (5.4 ± 3.4%)	113.1 ± 6.6 (10.8 ± 6.8%)	5.5 ± 1.8 (62 ± 70%)
Maximum during injection (% increase over baseline)	129.4 ± 14.6 (25.8 ± 13.6%)	132.4 ± 13.1 (29.6 ± 12.3%)	6.2 ± 1.9 (80.9 ± 57.5%)

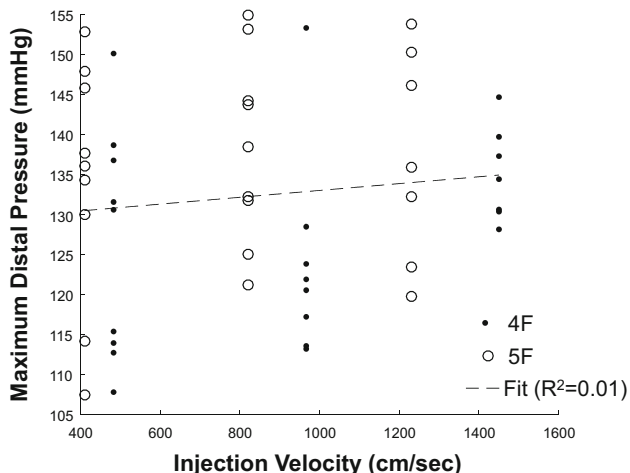


FIGURE 4. Maximum distal pressure during injection plotted against injection velocity in the pulsatile flow system. There is no correlation between the two variables. Values for both the 4F and 5F catheters are shown.

$n = 49$, $R^2 = 0.45$, $p < 1E-4$ for pulsatile flow). This correlation was stronger when the reflux length was normalized by the vessel diameter (Eq. 4).

$$\text{Correlation : Reflux Resistance} = C_1 \frac{L_{\text{reflux}}}{ID_{\text{vessel}}} + C_2 \tag{4}$$

Figure 5 shows the linear correlation of the reflux resistance and the normalized reflux length in both the steady flow and pulsatile flow systems. The steady flow system had a strong correlation ($n = 81$ samples, $R^2 = 0.82$, $p < 1E-4$, $C_{1,2} = 0.28, -0.14$) and the pulsatile flow system had a weaker correlation ($n = 49$, $R^2 = 0.56$, $p < 1E-4$, $C_{1,2} = 0.18, -0.74$) but still demonstrated a statistically significant linear behavior.

Figure 6 shows the correlation of the normalized reflux length and the Craya–Curtet number for each flow study. The behavior is representative of a sigmoidal function with an asymptotic leveling at lower

TABLE 3. Group differences and correlations of five different predictor variables (catheter size, vessel diameter, baseline blood flow rate, baseline distal pressure, and injection velocity) to two important response variables of the study (maximum distal pressure increase over baseline during injection and normalized reflux length).

	Distal pressure increase over baseline (mmHg)		Normalized reflux length	
	Steady flow	Pulsatile flow	Steady flow	Pulsatile flow
Catheter size	4F: 11.4 ± 2.7 5F: 16.0 ± 4.5 <i>p</i> < 0.0001	4F: 33.8 ± 12 5F: 26.5 ± 12.5 <i>p</i> = 0.045	4F: - 1.2 ± 3 5F: - 2.5 ± 4.2 <i>p</i> = 0.05	4F: - 2.4 ± 3.8 5F: - 4.4 ± 6.3 <i>p</i> = 0.45
Vessel diameter	4.8 mm: 15.6 ± 5 6.35 mm: 14 ± 3.7 8 mm: 12.2 ± 3.7 <i>p</i> = 0.011	4.8 mm: 30.8 ± 11.6 6.35 mm: 30.4 ± 9.3 8 mm: 29.5 ± 16.2 <i>p</i> = 0.98	4.8 mm: - 1.8 ± 5 6.35 mm: - 1.2 ± 2.6 8 mm: - 2.3 ± 3.2 <i>p</i> = 0.06	4.8 mm: - 2.7 ± 6.5 6.35 mm: - 3.5 ± 5.6 8 mm: - 3.8 ± 3.9 <i>p</i> = 0.1
Baseline blood flow	<i>R</i> ² = 0.002 <i>p</i> = 0.67	<i>R</i> ² = 0.005 <i>p</i> = 0.62	<i>R</i> ² = 0.42 <i>p</i> < 0.0001	<i>R</i> ² = 0.14 <i>p</i> = 0.009
Baseline distal pressure	<i>R</i> ² = 0.17 <i>p</i> < 0.0001	<i>R</i> ² = 3E-4 <i>p</i> = 0.9	<i>R</i> ² = 0.18 <i>p</i> < 0.0001	<i>R</i> ² = 0.11 <i>p</i> = 0.02
Injection velocity	<i>R</i> ² = 0.04 <i>p</i> = 0.08	<i>R</i> ² = 0.03 <i>p</i> = 0.26	<i>R</i> ² = 0.02 <i>p</i> = 0.22	<i>R</i> ² = 0.31 <i>p</i> < 0.0001

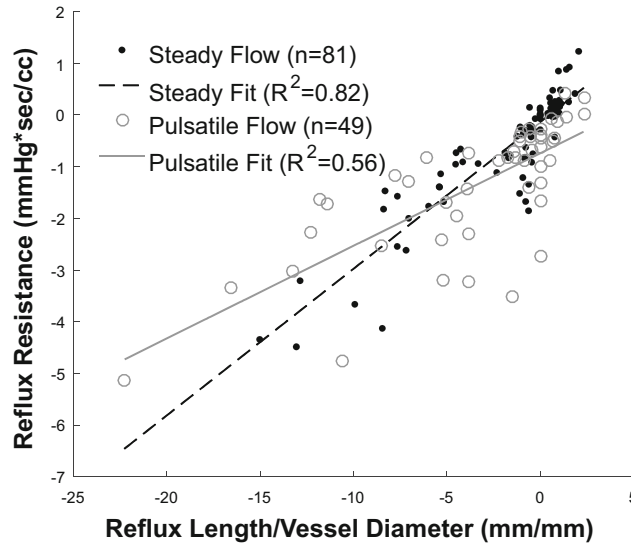


FIGURE 5. Plots of the Reflux Resistance parameter (see text for definition) against normalized reflux length for steady and pulsatile flow; linear regression lines are shown.

and higher Ct values. The data was fit to a logistic function seen in Eq. (5) with C_1, C_2, C_3, C_4 defining the constants of the function. The steady flow data showed a slightly weaker correlation ($n = 81, R^2 = 0.69, C_{1,2,3,4} = 0.42, 7.0, 0.84, 0.04$) as compared to pulsatile flow ($n = 49, R^2 = 0.85, C_{1,2,3,4} = 0.32, 2.8, 1.2, 0.06$).

$$\text{Correlation : } Ct = \frac{C_1}{\left(1 + C_2 e^{-\frac{C_3 L_{reflux}}{D_{vessel}}}\right)} + C_4 \quad (5)$$

The Reynolds numbers for the injections varied from 2200 to 7400, while the blood flow Reynolds numbers ranged from 20 to 420. Figure 7 shows the correlation of the logistic function to the ratio of Reynolds numbers and normalized reflux length

(Eq. 6). The correlation coefficients for the steady and pulsatile flow were 0.72 and 0.86, respectively (Steady flow: $n = 81, C_{1,2,3,4} = 0.18, 6.8, 0.83, 0.02$; Pulsatile flow: $n = 49, C_{1,2,3,4} = 0.16, 3.1, 1.1, 0.03$).

$$\text{Correlation : } \frac{Re_b}{Re_c} = \frac{C_1}{\left(1 + C_2 e^{-\frac{C_3 L_{reflux}}{D_{vessel}}}\right)} + C_4 \quad (6)$$

Anderson–Darling goodness-of-fit tests for these four logistic function fits (Ct and Re ratio for steady and pulsatile flow) showed that the residuals were normally distributed (p values > 0.06) for three of the four fits indicating a good fit; residuals for the pulsatile flow Re ratio vs. reflux length fit deviated from normality ($p = 0.03$).

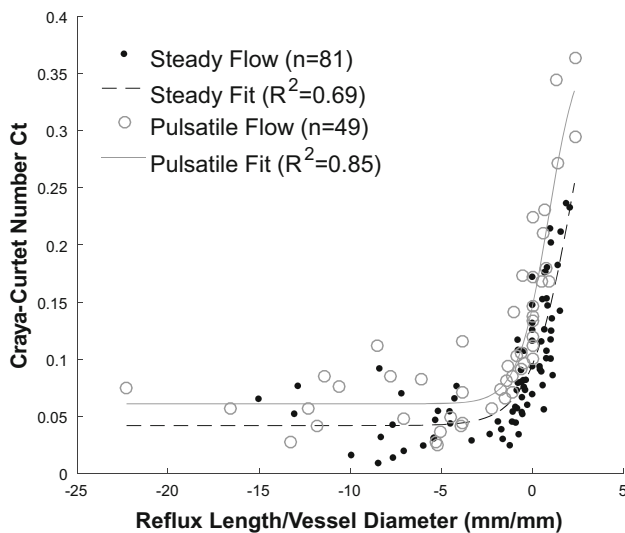


FIGURE 6. Plots of the non-dimensional Craya–Curtet number against normalized reflux length for steady and pulsatile flow; the lines show fits to the data with a logistic function.

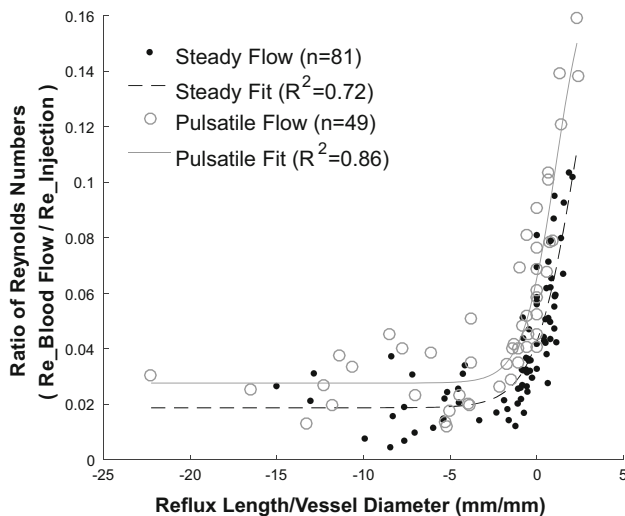


FIGURE 7. Plots of the non-dimensional ratio of Reynolds numbers against normalized reflux length for steady and pulsatile flow; the lines show fits to the data with a logistic function.

DISCUSSION

Contrast reflux has previously been evaluated in a few different contexts. The presence of contrast reflux into the jugular veins during CT or MR angiography has been correlated to suboptimal head and neck scan quality because of venous contrast density artifacts or delayed time of arrival of contrast to the region of interest; jugular vein reflux lengths have been measured to optimize the scan procedure.^{4,15} In general, contrast reflux is viewed as an excess or waste of contrast volume that does not contribute to image quality and the extent of reflux has been used as an indicator of the

quality of diagnostic angiography.⁹ Similarly, modified mechanical injectors that aim to minimize the volume of contrast injected while retaining image quality have used contrast reflux as a measure of excess.^{17,28} Severe contrast reflux into the inferior vena cava during pulmonary CT angiography has been suggested as a marker for right heart dysfunction.¹ Contrast reflux has been suggested to occur at the threshold where the rate of contrast injection exceeds the rate of blood flow¹⁰; a previous *in vivo* study²³ as well as our results here do not support this notion that reflux is simply related just to contrast injection or mean blood flow rates. Also, the pulsatility of flow is maintained in the distal segments during steady injection rates^{23,42} (Fig. 3) proving that the phenomenon is not a simplistic replacement of blood flow by contrast flow. Contrast reflux length into the inferior vena cava during coronary CT angiography has been linearly correlated to the tricuspid regurgitant jet velocity (and thus right ventricle systolic pressure) suggesting that reflux length can be representative of hemodynamic conditions.⁶ Our study is along the same lines as this last study. Our goal was not to optimize contrast injection parameters or the resultant image quality, but to study the hemodynamic conditions under which contrast reflux occurs during antegrade catheter-based arterial injections. Our results show that contrast reflux length is correlated to specific baseline and intra-injection parameters. We found two such correlations, which have not been reported previously and form the primary conclusions of our study.

First, the ratio of the distal to proximal pressure difference during injection and baseline flow rate, called the reflux resistance here, was linearly correlated to normalized reflux length (reflux length/vessel diameter). As stated, contrast injections generally involve high Reynolds number jets and the concomitant mixing with the co-flow of blood at and around the catheter tip are highly complex in cylindrical coordinates. Considering just the one-dimensional (along vessel axis) behavior, however, injections result in an increased pressure at/near the catheter tip with greater injection rates or volumes generating greater pressures. The injection thus temporarily changes the prevalent pressure gradients, where the pressure at the catheter-tip can increase above the distal as well as proximal pressures. The distal and proximal pressures also increase above the baseline pre-injection values; the rapid antegrade injection of fluid also implies that the increase in distal pressures can be more than the increase in proximal pressures. The proximal vascular resistance is dependent on the patient/system vascular geometry and hemodynamics and can thus be expected to remain constant for a given arterial segment. An increase in the backward pressure gradient (dis-

tal—proximal pressure) thus causes an effective ‘backflow’ which is visualized as reflux; the greater this pressure gradient, the greater the extent of reflux. We constructed a ‘reflux resistance’ parameter, which is the ratio of the pressure difference during injection to baseline flow rate, to represent this dynamic. The baseline flow rate is related to the proximal vascular resistance and the pressure difference during the injection is representative of the backward gradient that produces reflux. As can be expected based on the above description, there is a strong linear correlation between the reflux resistance and the reflux length (Fig. 5). Lower baseline flows or greater pressure gradients during injection result in a greater contrast ‘backflow’ or reflux length. It should be noted that while the occurrence of reflux and reflux length may be simply and linearly related to the pressure gradients during injection, the magnitude of the pressure increase during injection is the result of a complex interplay of the injection jet and coflowing blood (Fig. 4, Table 3).⁴² As such, local intra-injection pressure magnitudes cannot, for example, be derived by simple analysis of vascular resistances and baseline and injection flow rates. Assuming future testing and clinical validation show reliable accuracy, the significance of our result in Fig. 5 is that it provides a potential means to deduce intra-injection pressure gradients by simple measurement of the reflux length as visualized on angiograms.

Second, our results suggest a sigmoidal relationship between the reflux length and the Ct number and Re ratio. This relationship is also representative of the physics of contrast injections into co-flow, in that the two asymptotes of the function potentially highlight physical phenomena. With increasing Ct number (or Re ratio), the injection rate becomes smaller relative to the blood flow rate and the proximal edge of the mixing bolus extends farther downstream, *i.e.*, the efflux length increases. Asymptotically, as the injection rate becomes negligible, the injection becomes a laminar stream where the mixing of the contrast with the blood occurs through diffusion³⁹ and the efflux length is theoretically at infinity. With decreasing Ct numbers, the injection rate increases and the mixing occurs closer and closer to the catheter tip due to the large pressures and increasingly turbulent spread of the contrast jet at the injection site. Asymptotically, extremely high velocity injections into negligible or stagnant blood flow within a vessel set up severe reverse pressure gradients and the contrast refluxes such that the reflux length is theoretically at infinity. Again, future testing and clinical validation are required to show reliable accuracy, but Fig. 6 (or Fig. 7) can potentially be used to extract baseline arterial blood flow rates by the simple measurement of reflux length

on angiograms. A few caveats to the Ct number and Re ratio correlations may be noted—these two parameters are not independent and are essentially related given the flow and injection parameters. As mentioned, the goal of our study was to evaluate the conditions surrounding the occurrence of contrast reflux. Thus, we did not target a wide range of efflux lengths and the upper asymptote of the sigmoid functions are poorly defined. Additional studies with more efflux values need to be conducted to confirm whether the relationship to the Ct number and Re ratio is sigmoidal or some other function. Also, we chose the logistic function because it is comprised of an exponential function, which is commonly used to represent physical phenomena; we did not evaluate the goodness-of-fit of other sigmoid functions.

The 5–45 mmHg intra-injection pressure increases over baseline observed in this study are similar to those measured previously in *in vivo* and clinical studies.^{31,37,41,47} Coronary angiography through a 6F catheter in 25 patients with non-significant lesions resulted in a 6 ± 4.2 mmHg increase in proximal mean pressure at the coronary ostium.³⁷ Contrast injections at 5–10 cc/s through a 5F catheter placed in the proximal common carotid artery of dogs with pressure measurement *via* a catheter placed distally in the same vessel produced maximal pressure increases ranging from 40 to 125 mmHg.³¹ Contrast injections of 18 cc at 3 cc/s through a 5F catheter in the carotid or vertebral arteries of 25 patients showed pressure increases ranging from 3 to 54 mmHg (mean: 16 ± 13 mmHg, median ~ 20 mmHg) over the baseline; pressures were measured 2–3 cm distal to the catheter tip with a pressure wire.⁴¹

One limitation of our study relates to the large length (40 cm) of the test vessel, which is not physiologically correct. Distal and proximal pressures mentioned throughout the manuscript were measured 20 cm from the catheter tip. This vessel length was chosen so that the catheter could be placed at the midpoint, and the distal pressure sensor would be far enough to not record the pressure fluctuations within the contrast ejection and mixing zone. Also, the proximal pressure sensor needed to be far enough not to interfere with the angiographic imaging of long reflux lengths, which were up to 8 cm in some testing scenarios. A few extreme scenarios led to the contrast refluxing out of the field of view (data were discarded as the reflux lengths could not be measured). Additionally, the long test vessel helped demonstrate that substantial pressure increases can be generated during contrast injections over supra-physiological distances. The vascular compartment proximal to the catheter tip was limited to a tube here, but during clinical ante-grade injections, the proximal vascular compartment

will be much larger and hence the proximal pressure increases may be smaller in patients. However, as the angiographic region of interest is always distal to the catheter in antegrade injections, the distal pressure increases in the region of interest are far more crucial. Also, as stated above, our pressure increases fall within *in vivo* and clinically measured ranges. We did not find any correlations between the injection and baseline hemodynamics to the proximal or distal pressure magnitudes during injection or to the pressure increases over baseline, which further reinforces the fluid dynamic complexity of such contrast injections. For example, using the linear regression equation in Fig. 5, a reflux length of 1 cm visualized in the internal carotid artery could be translated to a 5 mmHg difference between the distal and proximal pressures, but we found no relationships (Table 3) to predict that proximal pressure may have possibly increased by 25 mmHg and distal pressure by 30 mmHg over the baseline; this can be seen in Table 2 where pressure increases over baseline are more substantial than the distal-to-proximal pressure differences. Establishing such a relationship could provide a simple tool to estimate distal pressure increases during injection, which can be crucial when imaging pathologies with weakened vascular walls like aneurysms.^{3,45} To this end, we plan to conduct a follow up study on silicone replicas of patient-specific aneurysm geometries.

We used a homogenous glycerol solution to mimic blood. While the particulate nature of blood³⁶ may need to be considered in studies of nano/micro-particle dispersions, iodinated contrast is essentially a chemical species and given the length and time scales of contrast reflux, the clinical significance of our results should not be effected by the use of a homogenous working fluid. Previous *in vitro* studies investigating contrast injections have also used homogenous working fluids.^{26,28} Again, the fact that our pressure increases are similar to *in vivo* and clinically measured values even when arterial blood or saline is used as the injectate^{21,42} validate the working fluid used. The injection volume (8 cc) used for the pulsatile system was different than that used for the steady flow system (4 cc) because our goal was to produce contrast reflux and the pulsatile system had higher ranges of baseline flows. The chosen injection volumes resulted in a similar range of reflux lengths in both systems. In other words, a 4 cc injection volume in the pulsatile system would have potentially resulted in data points limited to a narrow range around zero reflux length (Figs. 5,6 and 7), or a 8 cc injection in the steady flow system would have potentially resulted in only large (negative) reflux lengths. The 8 cc injection volume in the pulsatile system is within the range of clinically used volumes in the internal carotid artery (7.9 ± 1.5 cc).⁴⁵ However, it

should be noted that the differences between the maximum and average distal pressures and reflux lengths mentioned above or the differences in the correlation constants (Figs. 5,6 and 7) between the steady and pulsatile flow systems could potentially be due to the different injection volumes. We used an equivalent range of injection rates (3–9 cc/s) in both systems, but differing injection volumes to ensure a similar range of reflux lengths, and hence the time period of injections was different. The reflux resistance, ratio of Reynolds numbers or the Craya–Curtet number do not account for the time period, so further studies need to be conducted with different injection volumes to determine the effect of injection time. The hydraulic resistance of the steady and pulsatile systems was also different and this may have contributed to the differences; future testing of steady and pulsatile flow in identical benchtop setups would help mitigate this variable.

Similarly, although we chose vessel diameters and catheter sizes relevant to cerebral angiography, future studies could be conducted with a wider range of vessel diameters, lengths, or catheter sizes. The ordinate values in the correlations shown in this study (Figs. 5, 6 and 7) contain the baseline blood flow rate as a variable. Although the baseline distal pressure did not correlate to the distal pressure increase in the pulsatile flow system, it can be speculated that some link exists between the baseline distal pressure and the pressure increases at the catheter tip during injection, which in turn would cause greater reflux. These might explain the very weak correlations we found (Table 3) between the baseline blood flow rate and baseline distal pressure to the normalized reflux length. In general, however, we found no obvious relationship between reflux and initial systemic pressures, injection rates, catheter sizes, or vessel diameters (Table 3). We collected data under 81 different conditions in the steady flow system and 49 different conditions in the pulsatile system. The steady flow experiments were conducted first and involved a more detailed investigation of the variables. Specifically, we investigated many increments of baseline pressures and five different injection rates. The number of conditions for the pulsatile flow experiments were then reduced (specifically, baseline pressures and injection rates) based on the results of the steady flow experiments. The fact that there were 81 conditions for the steady flow and 49 conditions for the pulsatile flow has no bearing on the final results and conclusions of the study. The effect of side-branches was not studied here and such branches may substantially change the hemodynamics during injections. Overall, while our study contains some parameter assumptions and limitations, the large sample size and detailed data collection firmly establish the relation-

ships seen between the reflux lengths and reflux resistance, momentums, and forces.

The potential clinical utility of our results lies in the two correlations—the linear relation between the reflux resistance and the reflux length and the sigmoidal relation between the Ct number (or Re ratio) and the reflux length. The coefficients of the correlations are potentially system-specific constants and may vary from patient-to-patient. Moreover, the accuracy of the trends shown here need to be verified in the clinical scenario. Under pulsatile flow, the correlation coefficients for the sigmoid function fits were reasonably high ($R^2 \sim 0.85$ for the Ct and Re ratio) while that for the linear fit to reflux resistance was moderate ($R^2 = 0.56$). The average error between the actual/measured baseline flow rate and the estimated flow rate as given by the sigmoid function was 0.2 ± 1 cc/s (actual baseline flow ranged from 1.5 to 6 cc/s); the error between the actual pressure difference during injection and that estimated by the linear fit was -0.6 ± 3.3 mmHg (actual pressure difference ranged from -18 to 2.2 mmHg). Thus, in this benchtop study, the prediction accuracy for the flow rates was better than that for the pressure difference. The addition of angiography viewing plane, three-dimensionality of vasculature, cardiac cycle variability, *etc.*, could potentially add to the measurement uncertainty of using these trends to estimate baseline flow rates or pressure differences during injections in patients. Further *in vivo* and possibly prospective clinical studies are needed in order to generate a family of response curves, establish a robust confidence interval for the coefficients, and obtain reliable estimation accuracy in patients. As reflux is dependent on the proximal and distal vascular hydraulic resistance, it may be reasonable to expect that the steady flow system used here (steady flow curves in Figs. 5, 6, and 7) represents a lower bound for the coefficients. If such a confidence interval is established with future studies, the sigmoid functions could be used to extract baseline mean blood flow rates in any artery of interest in any patient. For example, 3–5 injections at different rates can be made with any catheter in the vessel and the vessel diameter and reflux or efflux lengths can be measured on the angiograms. The mean blood flow rate is the only unknown parameter in the Ct number. Thus, using the established confidence intervals of the sigmoid function coefficients, the mean flow rate of the artery can be quantified with given precision. It would be valuable to be able to extract the distal pressure increase over the baseline based on the baseline and injection parameters, but we found no obvious correlations to the pressure magnitudes. The mean intra-injection proximal-to-distal pressure gradient could, however, be quantified in any patient using the same method-

ology as mentioned above for the baseline arterial flow rate. The distal pressure during injection could then be quantified if the pressure proximal to the injection catheter were measured. The linear correlation between the reflux resistance and reflux length can also be used to avoid scenarios where the distal pressure increases above the proximal pressure. For example, using the pulsatile system correlation coefficients in Fig. 5 and assuming a vessel diameter of 9, 5, and 3 mm for the common carotid, internal carotid, and vertebral arteries, contrast injections in these vessels should have an efflux length of at least 4, 2, and 1.2 cm to ensure that the distal pressure remains lower than the proximal pressure.

CONCLUSIONS

Catheter-based angiography can result in substantial increases in local flows and pressures over the corresponding pre-injection values as also described by previous studies. On average, we recorded 45–80% increases in flow and 30–50% increases in pressure over baseline values. These increases can occur at large distances distal to the catheter tip and thus care must be exercised during contrast injections to diagnose or treat weak-walled pathologies such as aneurysms. Given the tested conditions (Table 1), three important conclusions can be derived from this study:

- i. Contrast reflux occurs when the pressure distal to the catheter tip increases above the proximal pressure during injections. The difference between the distal and proximal pressure can be expected to be minimal (~ 5 – 10 mmHg) in standard cerebral angiography.
- ii. The ratio of this pressure difference to baseline flow rate is linearly correlated to the ratio of the contrast reflux/efflux length to vessel diameter.
- iii. The ratio of blood and contrast fluid momentums and the ratio of blood and contrast Reynolds numbers are correlated to the ratio of the contrast reflux/efflux length to vessel diameter potentially *via* sigmoid functions.

These solutions were found to describe both steady and pulsatile flow scenarios and are thus potentially representative of catheter based injections in patients. As the abscissa (ratio of reflux/efflux length to vessel diameter) can be measured in any patient, patient-specific hemodynamics can be extracted if the accuracy of the linear and sigmoid functions described here are firmly quantified by future studies. The flow and injection rates used in this study are relevant to neuro-

angiography, but the results should be essentially applicable to antegrade injections in peripheral angiography as well.

ELECTRONIC SUPPLEMENTARY MATERIAL

The online version of this article (<https://doi.org/10.1007/s13239-018-0344-3>) contains supplementary material, which is available to authorized users.

CONFLICT OF INTEREST

Author BK is partly employed by Vascular Simulations LLC. All other authors have stock ownership in Vascular Simulations LLC.

HUMAN/ANIMAL STUDIES

No human or animal studies were carried out by the authors for this article.

REFERENCES

- ¹Aviram, G., D. Cohen, A. Steinvil, H. Shmueli, G. Keren, S. Banai, *et al.* Significance of reflux of contrast medium into the inferior vena cava on computerized tomographic pulmonary angiogram. *Am. J. Cardiol.* 109(3):432–437, 2012. <https://doi.org/10.1016/j.amjcard.2011.09.033>.
- ²Becker, H. A. Discussion: “Confined jet mixing for non-separating conditions” (Razinsky, E., and Brighton, JA, 1971, ASME J. Basic Eng., 93, pp. 333–347). *J. Basic Eng.* 93(3):347, 1971.
- ³Celtikci, P., O. Eraslan, O. Ergun, E. Soyer Guldogan, and M. E. Turkoglu. Active rebleeding from a ruptured middle cerebral artery aneurysm during diagnostic catheter angiography. *Turk Neurosurg.* 2017. <https://doi.org/10.5137/1019-5149.jtn.19629-16.2>.
- ⁴Demirpolat, G., M. Yuksel, G. Kavukcu, and D. Tuncel. Carotid CT angiography: comparison of image quality for left versus right arm injections. *Diagn. Interv. Radiol.* 17(3):195–198, 2011. <https://doi.org/10.4261/1305-3825.dir.3290-10.1>.
- ⁵Dublin, A. B., and B. N. French. Cerebral aneurysmal rupture during angiography with confirmation by computed tomography: a review of intra-angiographic aneurysmal rupture. *Surg. Neurol.* 13(1):19–26, 1980.
- ⁶Dusaj, R. S., K. C. Michelis, M. Terek, R. Sanai, R. Mittal, J. F. Lewis, *et al.* Estimation of right atrial and ventricular hemodynamics by CT coronary angiography. *J Cardiovasc Comput Tomogr.* 5(1):44–49, 2011. <https://doi.org/10.1016/j.jcct.2010.10.005>.
- ⁷Endres, J., Redel, T., Kowarschik, M., Hutter, J., Hornegger, J., Doerfler, A. (eds.). Virtual angiography using CFD simulations based on patient-specific parameter optimization. In: 2012 9th IEEE International Symposium on Biomedical Imaging (ISBI), IEEE, 2012.
- ⁸Ford, M. D., G. R. Stuhne, H. N. Nikolov, D. F. Habets, S. P. Lownie, D. W. Holdsworth, *et al.* Virtual angiography for visualization and validation of computational models of aneurysm hemodynamics. *IEEE Trans. Med. Imaging* 24(12):1586–1592, 2005.
- ⁹Genereux, P., R. Mehran, M. B. Leon, N. Bettinger, and G. W. Stone. Classification for assessing the quality of diagnostic coronary angiography. *J. Invasive Cardiol.* 29:417–420, 2017.
- ¹⁰Gianturco, C., T. Shimizu, F. R. Stefferda, and R. P. Taylor. Measurement of blood flow by angiography with increasing rate of injection: experimental study. *Investig. Radiol.* 5(5):361–363, 1970.
- ¹¹Hao, Q., and B. B. Lieber. Dispersive transport of angiographic contrast during antegrade arterial injection. *Cardiovasc. Eng. Technol.* 3(2):171–178, 2012.
- ¹²Hayakawa, K., T. W. Morris, R. W. Katzberg, and H. W. Fischer. Cardiovascular responses to the intravertebral artery injection of hypertonic contrast media in the dog. *Investig. Radiol.* 20(2):217–221, 1985.
- ¹³Henriksen, J. H., G. B. Jensen, and H. B. Larsson. A century of indicator dilution technique. *Clin. Physiol. Funct. Imaging* 34(1):1–9, 2014. <https://doi.org/10.1111/cpf.12068>.
- ¹⁴Hilal, S. K. Hemodynamic changes associated with the intra-arterial injection of contrast media. New toxicity tests and a new experimental contrast medium. *Radiology* 86(4):615–633, 1966. <https://doi.org/10.1148/86.4.615>.
- ¹⁵Hingwala, D. R., B. Thomas, C. Kesavadas, and T. R. Kapilamoorthy. Suboptimal contrast opacification of dynamic head and neck MR angiography due to venous stasis and reflux: technical considerations for optimization. *AJNR Am. J. Neuroradiol.* 32(2):310–314, 2011. <https://doi.org/10.3174/ajnr.A2301>.
- ¹⁶Huang, B., J. Chang, C. Wang, and V. Petrenko. A 1-D analysis of ejector performance. *Int. J. Refrig.* 22(5):354–364, 1999.
- ¹⁷Kaye, D. M., D. Stub, V. Mak, T. Doan, and S. J. Duffy. Reducing iodinated contrast volume by manipulating injection pressure during coronary angiography. *Catheter. Cardiovasc. Interv.* 83(5):741–745, 2014. <https://doi.org/10.1002/ccd.25348>.
- ¹⁸Keenan, J. H., E. P. Neumann, and F. Lustwerk. An investigation of ejector design by analysis and experiment. Cambridge, MA: Massachusetts Institute of Technology, Guided Missiles Program, 1948.
- ¹⁹Kusumi, M., M. Yamada, T. Kitahara, M. Endo, S. Kan, H. Iida, *et al.* Rerupture of cerebral aneurysms during angiography—a retrospective study of 13 patients with subarachnoid hemorrhage. *Acta Neurochir. (Wien)* 147(8):831–837, 2005. <https://doi.org/10.1007/s00701-005-0541-3>.
- ²⁰Levin, D. C. Augmented arterial flow and pressure resulting from selective injections through catheters: clinical implications. *Radiology* 127(1):103–108, 1978. <https://doi.org/10.1148/127.1.103>.
- ²¹Levin, D. C., D. A. Phillips, S. Lee-Son, and P. R. Maroko. Hemodynamic changes distal to selective arterial injections. *Investig. Radiol.* 12(2):116–120, 1977.
- ²²Lieber, B. B., C. Sadasivan, M. J. Gounis, J. Seong, L. Miskolczi, and A. K. Wakhloo. Functional angiography. *Crit. Rev. Biomed. Eng.* 33(1):1–102, 2005.
- ²³Lieber, B. B., C. Sadasivan, Q. Hao, J. Seong, and L. Cesar. The mixability of angiographic contrast with arterial

- blood. *Med. Phys.* 36(11):5064–5078, 2009. <https://doi.org/10.1118/1.3243079>.
- ²⁴Mabon, R. F., P. D. Soder, W. A. Carpenter, and D. P. Giddens. Fluid dynamics in cerebral angiography. *Radiology* 128(3):669–676, 1978. <https://doi.org/10.1148/128.3.669>.
- ²⁵Morris, T. W., M. Francis, and H. W. Fischer. A comparison of the cardiovascular responses to carotid injections of ionic and nonionic contrast media. *Investig. Radiol.* 14(3):217–223, 1979.
- ²⁶Morris, T. W., and C. S. Walike. An in vitro study of the hemodynamic effects of catheter injections. *Investig. Radiol.* 24(5):361–365, 1989.
- ²⁷Mulder, G., A. Bogaerds, P. Rongen, and F. van de Vosse. The influence of contrast agent injection on physiological flow in the circle of Willis. *Med. Eng. Phys.* 33(2):195–203, 2011.
- ²⁸Prasad, A., C. Ortiz-Lopez, D. M. Kaye, M. Byrne, S. Nanayakkara, S. H. Ahmed, *et al.* The use of the AVERT system to limit contrast volume administration during peripheral angiography and intervention. *Catheter. Cardiovasc. Interv.* 86(7):1228–1233, 2015. <https://doi.org/10.1002/ccd.26155>.
- ²⁹Razinsky, E., and J. Brighton. Confined jet mixing for nonseparating conditions. *J. Basic Eng.* 93(3):333–347, 1971.
- ³⁰Rosengarten, B., M. K. Steen-Muller, A. Muller, H. Traupe, R. K. Voss, and M. Kaps. Contrast media effect on cerebral blood flow regulation after performance of cerebral or coronary angiography. *Cerebrovasc. Dis.* 16(1):42–46, 2003.
- ³¹Saitoh, H., K. Hayakawa, K. Nishimura, Y. Okuno, C. Murayama, T. Miyazawa, *et al.* Intracarotid blood pressure changes during contrast medium injection. *AJNR Am. J. Neuroradiol.* 17(1):51–54, 1996.
- ³²Saitoh, H., K. Hayakawa, K. Nishimura, Y. Okuno, T. Teraura, K. Yumitori, *et al.* Rupture of cerebral aneurysms during angiography. *Am. J. Neuroradiol.* 16(3):539–542, 1995.
- ³³Sampei, T., N. Yasui, M. Mizuno, S. Nakajima, T. Ishikawa, H. Hadeishi, *et al.* Contrast medium extravasation during cerebral angiography for ruptured intracranial aneurysm; clinical analysis of 26 cases. *Neurol. Med. Chir.* 30(13):1011–1015, 1990. <https://doi.org/10.2176/nmc.30.1011>.
- ³⁴Shpilfoygel, S. D., R. A. Close, D. J. Valentino, and G. R. Duckwiler. X-ray videodensitometric methods for blood flow and velocity measurement: a critical review of literature. *Med. Phys.* 27(9):2008–2023, 2000. <https://doi.org/10.1118/1.1288669>.
- ³⁵Singh, G. Entrainment and mixing studies for a variable density confined jet. *Numer. Heat Transf. Part A Appl.* 35(2):205–224, 1999.
- ³⁶Skorczewski, T., L. C. Erickson, and A. L. Fogelson. Platelet motion near a vessel wall or thrombus surface in two-dimensional whole blood simulations. *Biophys. J.* 104(8):1764–1772, 2013.
- ³⁷Stoel, M., J. Kandhai-Ragunath, G. Van Houwelingen, and C. Von Birgelen. Impact of dye injection on intracoronary pressure. *EuroIntervention* 5(2):272–276, 2009.
- ³⁸Sun, Q., A. Groth, and T. Aach. Comprehensive validation of computational fluid dynamics simulations of in vivo blood flow in patient-specific cerebral aneurysms. *Med. Phys.* 39(2):742–754, 2012. <https://doi.org/10.1118/1.3675402>.
- ³⁹Taylor, G. Dispersion of soluble matter in solvent flowing slowly through a tube. *Proc. R. Soc. Lond. Ser. A Math. Phys. Sci.* 219(1137):186, 1953.
- ⁴⁰Vali, A., A. A. Abla, M. T. Lawton, D. Saloner, and V. L. Rayz. Computational Fluid Dynamics modeling of contrast transport in basilar aneurysms following flow-altering surgeries. *J. Biomech.* 50:195–201, 2017.
- ⁴¹Waldenberger, P., A. Chemelli, and A. Mallouhi. Intra-arterial haemodynamic changes during cerebral three-dimensional rotational angiography. *Eur. Radiol.* 19(2):503–508, 2009. <https://doi.org/10.1007/s00330-008-1161-0>.
- ⁴²Wolf, G. L., D. D. Shaw, H. A. Baltaxe, K. Kilzer, and L. Kraft. A proposed mechanism for transient increases in arterial pressure and flow during angiographic injections. *Investig. Radiol.* 13(3):195–199, 1978.
- ⁴³Woodfield, P. L., Nakabe, K., Suzuki, K. (eds.). Numerical computation on recirculation flow structures in co-axial confined laminar jets. In: 14th Symposium on Computational Fluid Dynamics 2000. Japan: Japanese Society of Fluid Mechanics.
- ⁴⁴Yamashita, K., K. Hayakawa, M. Tanaka, and J. Konishi. Cardiovascular responses following the intracarotid injections of ionic and nonionic contrast media compared with various mannitol solutions. *Correl. Osmolality Investig. Radiol.* 23(9):680–686, 1988.
- ⁴⁵Yousem, D. M., and B. C. Trinh. Injection rates for neuroangiography: results of a survey. *AJNR Am. J. Neuroradiol.* 22(10):1838–1840, 2001.
- ⁴⁶Yule, A., and M. Damou. Investigations of ducted jets. *Exp. Therm Fluid Sci.* 4(4):469–490, 1991.
- ⁴⁷Zaehring, M., C. Wedekind, A. Gossmann, K. Krueger, G. Trensche, and P. Landwehr. Aneurysmal re-rupture during selective cerebral angiography. *Eur. Radiol.* 12(Suppl 3):S18–S24, 2002. <https://doi.org/10.1007/s00330-002-1460-9>.